

PARAMETRIC ANALYSIS OF SOLAR PHOTOVOLTAIC MODULES AND IMPROVISATION THROUGH REAL TIME TESTING

Aniket Anand Anshul Rathie Saman Zia Kushal Koirala

Sustainable Energy Engineering Department, Indian Institute of Technology, Kanpur

Abstract

In the global transition to sustainable power sources, solar PV modules are essential for capturing clean, renewable energy from the sun. These modules greatly minimize the need for fossil fuels, reduce their negative effects on the environment, and combat climate change by converting solar energy into electrical energy. The performance of a solar PV system is influenced by several factors, these include the arrangement of modules in series and parallel, the effects of radiation through halogen lights, temperature, tilt angle shading effects, and the surface temperature of the solar module. This report focuses on analyzing how these parameters impact the efficiency and maximum power output of the solar PV system and then real time testing of the solar modules has been done based on single or double axis tracking system using microcontroller. Concept of solar altitude and solar azimuth angle variation has been used in the background theory of it. Kanpur location has been used for overall analysis of the same.

I. Introduction

In recent years, combination of scientific advancements, falling material costs, and government backing for power production from renewable sources has resulted in a rapid growth in solar photovoltaic (PV) technology. Moreover, the need for sustainable energy sources has led to a growing demand for renewables, including solar photovoltaic systems that can efficiently capture and use solar radiation without any environmental harm. Although solar PV has many advantages, it has several challenges, including low energy conversion efficiency, limited availability during the day, and unpredictability due to

weather variations. So, to overcome the challenges associated with PV and make the most use of the solar PV system, a thorough analysis of the several variables that directly affect output power, such as radiation, temperature, tilt angle, shading, and so on, is crucial [1].

Out of several factors affecting the performance of solar PV, radiation is considered to be one of the main factors because it acts as a fuel for solar PV. The amount of radiation received on the solar panel is to be converted into electrical energy. Hence, radiation has a significant influence on the output power of the solar PV panel. To install solar PV, a proper analysis of the effects of radiation is desired because the radiation level in specific locations changes throughout the day, and different geographical locations and climates also affect the radiation. With the increase in radiation level, the output power of the solar PV also increases [2], which will be experimentally validated in this work.

Temperature is critical factor that influences the performance of solar PV. With the increase in the solar panel's temperature, the short circuit current rises, and the open circuit voltage decreases; thus, the efficiency decreases [3]. Therefore, efficient temperature control of PV module is necessary for the proper functioning of solar power systems. The tilt angle and inclination of a photovoltaic system considerably influence its performance. Studies have indicated that as tilt angle increases, open-circuit voltage and short-circuit current decrease substantially, whereas the fill factor drops gradually [4].

Shading is another factor that significantly affects the performance of the PV module. For example, when a passing cloud or nearby buildings shade a PV panel, the result is not only energy loss during conversion but also additional non-linearity in the I-V characteristics [5]. Cell breakdowns may occur if there is no protection, which is why a bypass diode is typically utilized to safeguard the module. Large energy losses can occur from shadowing in a PV array configuration, and the energy yield can be significantly impacted by even tiny shadows [6].

II. Experimental Method

A) Experimental set-up

The experimental setup is depicted in Figure 1. The description of each component is as follows:

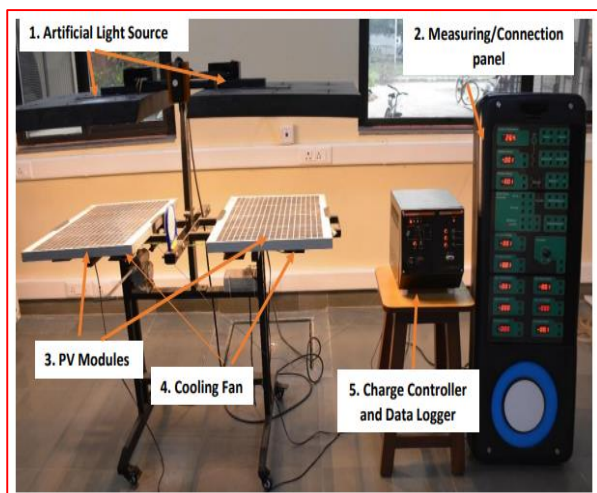


Figure 1. Experimental Setup

• PV Module:

Two P-V module setups (polycrystalline), of rating 40W, $V_{oc} = 21.60$ V, $V_m = 17.80$ V, $I_m = 2.25$ A each.

A module consists of several solar cell strings (fundamental building blocks) sealed between the layers of EVA (ethyl vinyl acetate), and they are arranged as per our requirement in series or parallel.

• Artificial Light Source:

It is challenging to manage sunlight in the lab, so we have to use an artificial lamp made up of halogen because there is a comparison of the halogen spectra to the solar and blackbody spectrums at 5500 K.

The PV module experiences solar radiation at an intensity of 110 to 330 W/m², corresponding to the solar radiation falling on the module within its spectral range.

Parallel radiation is hitting the PV modules. Consequently, we employ twelve 150-watt halogen bulbs instead of one 1800-watt halogen lamp. A 4x 3 aspect ratio is used to arrange the modules to generate uniform radiation.

• Measuring/Connection Panel:

It consists of various meters like an ammeter, which measures current flow; a voltmeter, which tells potential differences; and a thermocouple for temperature measurement. A Charge controller unit and an Inverter of 50W rating convert DC to AC converter. There are also two batteries with ratings of 4.5 Ah, each having 12V. AC and DC loads are also there.

• Cooling Fan:

During operation, the PV module tends to heat up, which alters its efficiency. Therefore, eight DC centrifugal (blower/squirrel-cage) fans are employed to cool the modules.

• Charge Controller Unit:

It consists of two units.

i. Converter unit: This system has a DC-DC converter with a 25-watt power rating, a nominal voltage of 12 volts, and a maximum load current rating of 2 A. Depending on the situation, it can operate in Manual or Auto mode.

ii. Data logger-plotter unit: The I-V and P-V characteristics can be plotted straight into

a computer using a data logger-plotter with the software ECOSENSE.

B) Experimental Procedure

1. I-V and P-V characteristics of PV modules with Varying radiation and temperature level

The first step in the process is to identify and connect the control board's components in accordance with the circuit diagram as shown in figure 2.1. After that, the plotter unit and the computer are connected via a Serial bus cable (RS-232) to record and store the data collected from the solar panels. The module or array output is connected to the ports of the plotter unit that correspond to the current and voltage sensors.

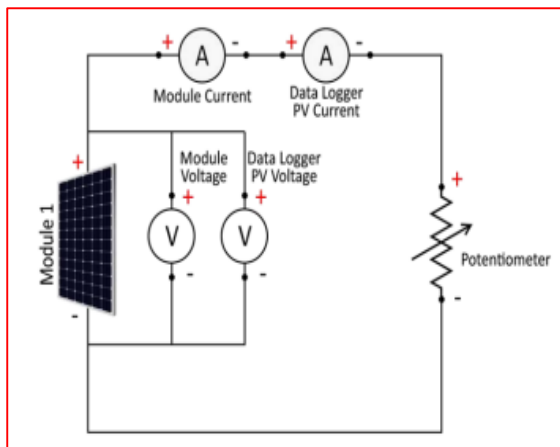


Figure 2.1: Effect of radiation

With the help of pyranometer, the radiation level was adjusted as per desire value. the mean of three measurements obtained from three distinct spots on the panel i.e. at top, bottom and on middle, with a radiation level of 110 W/m^2 , 220 W/m^2 , 330 W/m^2

The potentiometer was set to the maximum value in order to determine the open-circuit voltage (V_{oc}), short-circuit current (I_{sc}), and maximum power point (MPP) of the solar panels. The data for $V=V_{oc}$, current I , and power were then recorded.

Load was varied using the potentiometer to obtain the I-V and P-V characteristics of the solar panels. After recording of the data, I-

V and P-V characteristics were plotted using the data obtained.

2. I-V and P-V characteristics of series and parallel combinations of PV modules.

In order to carry out this experiment, the control board was initially connected in series and subsequently in parallel as shown in the figure 2.2 and 2.3. Next, the output from the solar panel module connected to the ports on the plotter unit for the voltage and current sensors. The PC and plotter unit were linked together using an RS-232 serial bus cable. Using a pyranometer (average of three separate sites on the module), the radiation level was set to roughly 110 W/m^2 , then repeat it for 220 W/m^2 , 330 W/m^2 .

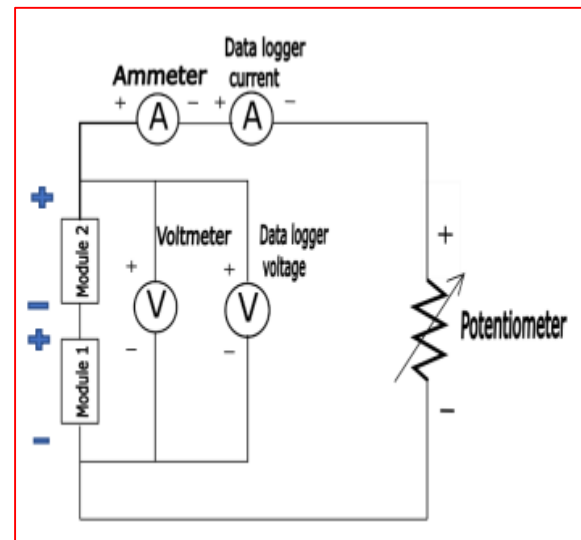


Figure 2.2: Series connected PV module

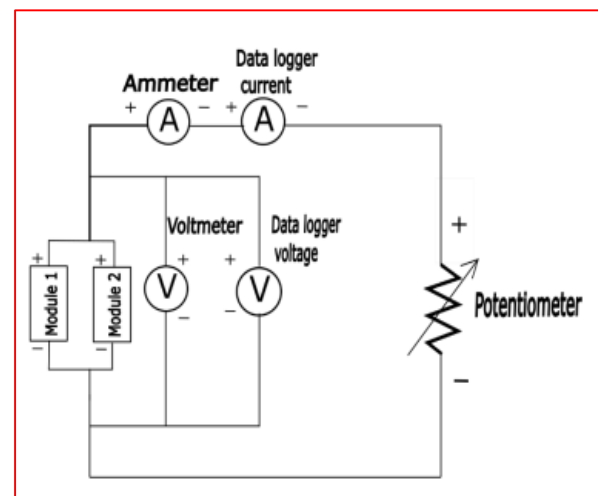


Figure 2.3: Shunt connected PV module

3. Effect of change in tilt angle on the output of PV modules.

We connected the components as the circuit schematic indicated in figure 2.4 then placed the inclinometer and first set the angle at 0 degree then vary angle to see its effect. Here, we maintain our radiation at 330W/m^2 .

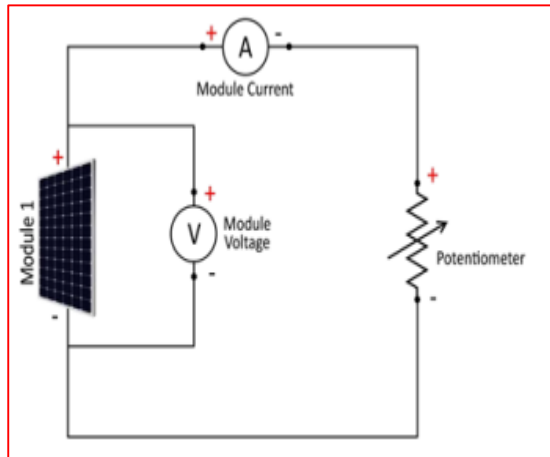


Figure 2.4. Effect of tilt angle

4. Effect of shading on module output power

Firstly, we make connection as mention in figure 2.5 without using bypass diode, and take readings at 330W/m^2 after that take reading with bypass diode as shown in figure 2.6.

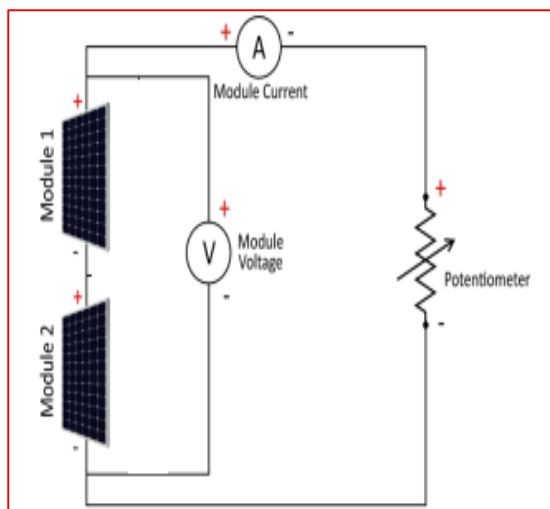


Figure: 2.5 Without bypass diode

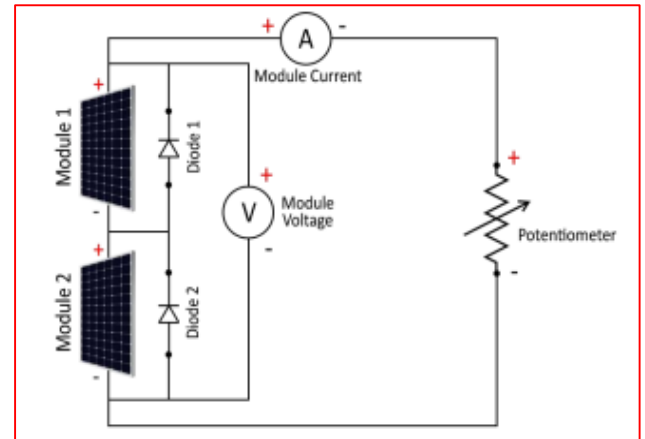


Figure: 2.6 With bypass diode

5. Function of a blocking diode.

Connect the battery, LED, and PV module without any blocking diodes as shown in the figure 2.7 at 330W/m^2 . Now cover the module completely so that module output becomes zero, LED will glow then use blocking diode as shown in figure 2.8, LED will stop glowing.

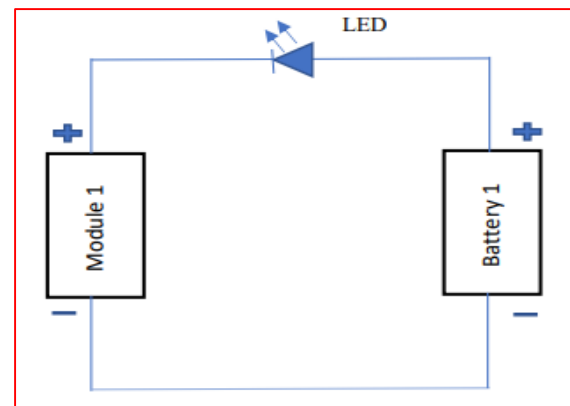


Figure 2.7: Without blocking diode

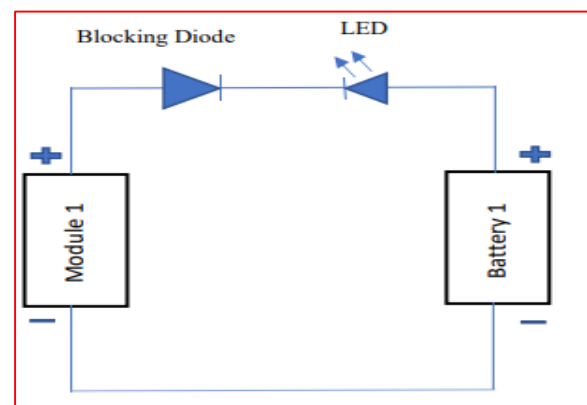


Figure 2.8. With blocking diode

6. Effect of Temperature on efficiency of module.

To observe the effect of temperature on the PV module first connect the PV module as shown in figure 2.9. After making this, we set the average radiation $\approx 330 \text{ W/m}^2$. Set the load resistance (potentiometer) setting to a Specific value & note down the readings of V and I with every change in temperature.

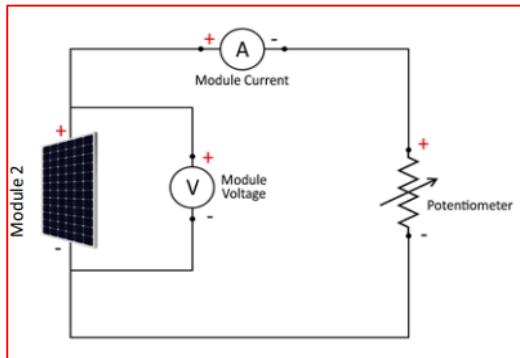


Figure: 2.9 Circuit diagram to observe the effect of temperature

III. Discussions of the existing setup:

The performance of PV module for three different values of irradiance were obtained by following the procedure mentioned in previous section. For the first experiment, I-V and P-V characteristics has been obtained as depicted in the figure 3.1 and 3.2 respectively.

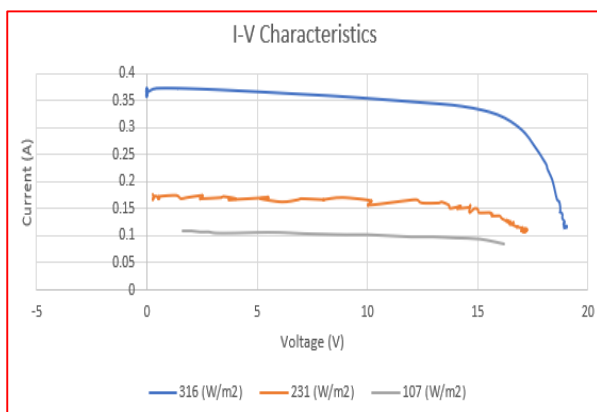


Figure 3.10 I-V Characteristics of PV module

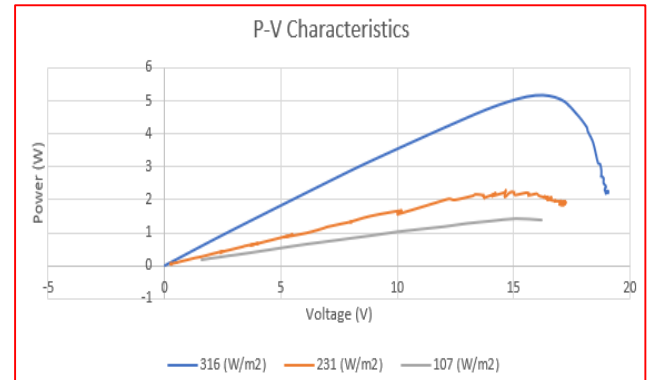


Figure 3.2 P-V Characteristics of PV module

The characteristics of I_{sc} and V_{oc} for different radiation values is shown in the figure 3.3 and 3.4 respectively. So, it can be observed that with the increase in the radiation value the I_{sc} increases due to the reason that there is increase in charge carrier inside the valance band of PV materials. V_{oc} also increases slightly since there is variation in external parameters such as ambient temperature, but V_{oc} should not be changed ideally. It can also be observed that the maximum power point increases with the increase in the radiation intensity.

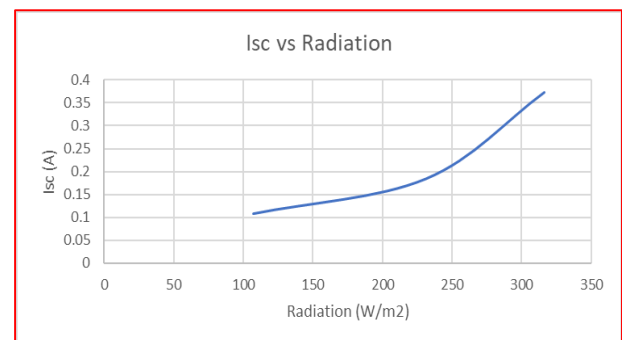


Figure 3.3 I_{sc} vs radiation of PV module

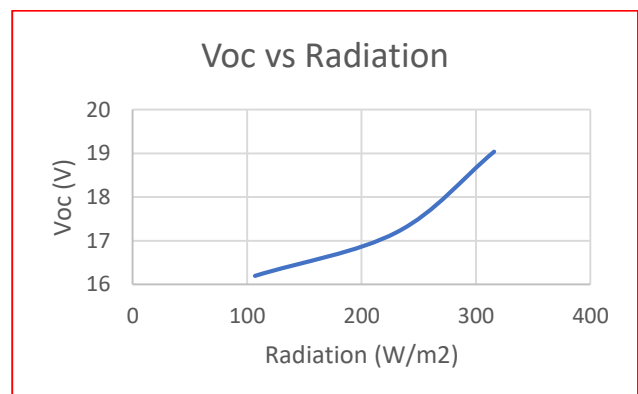


Figure 3.4 V_{oc} vs radiation of PV module

Similar to the first experiment, the performance of the series and parallel connection of the PV modules were observed. Figure 3.5 and Figure 3.6 shows the I-V and P-V characteristics of the series connected PV module for different values of radiation. Similarly, I-V and P-V characteristics of the parallel connected PV module is shown in the figure 3.7 and 3.8 respectively. It is observed that when two modules are connected in parallel, the voltage across each terminal is the same, and the current is added across the two terminals, increasing the overall current through the system so, I_{sc} increases. In a series connection, the current is constant and the combined V_{oc} of the two modules results in a higher V_{oc} . Also, P_{max} is the function of V_m and I_m .

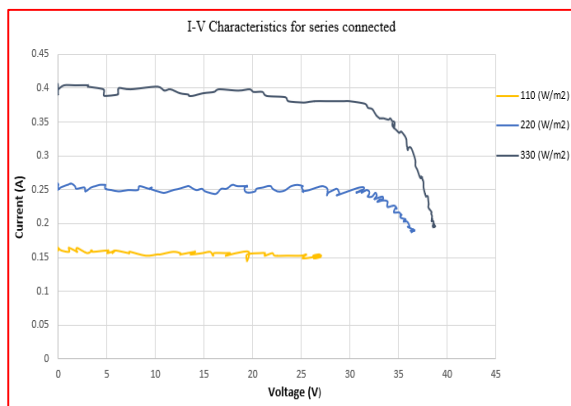


Figure 3.5. I-V Characteristics of series connected PV module

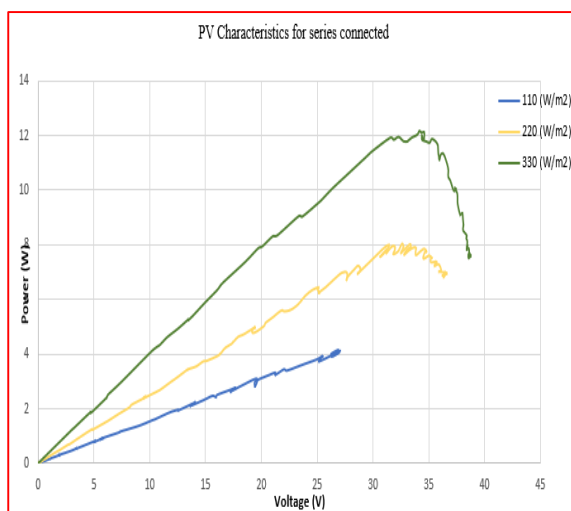


Figure 3.6. P-V Characteristics of series connected PV module

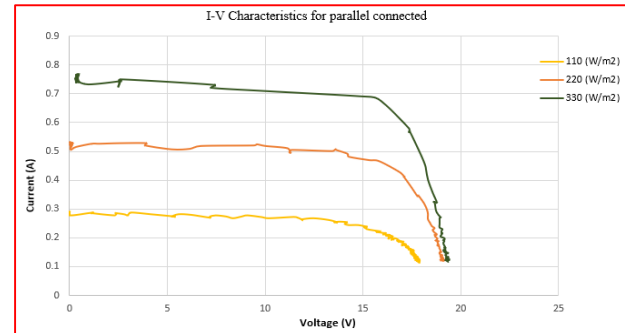


Figure 3.7. I-V Characteristics of parallel connected PV module

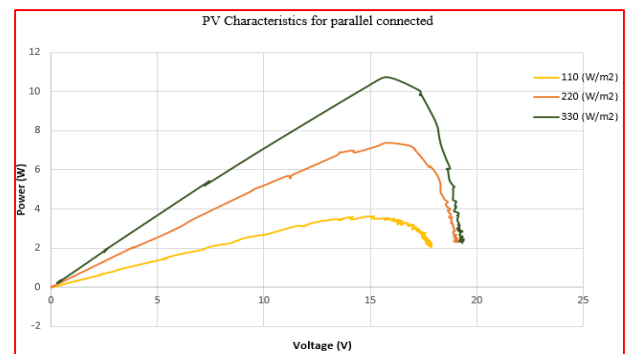


Figure 3.8. PV characteristics of parallel connected PV module

In our analysis, we saw that power is at its maximum (approximately 5W) when the tilt angle is 0 degrees, and it decreases with the increase in the tilt angle, as shown in figure 3.9. We deduced from this data that the PV module's output changes according to the season and time of day. In summer, in midday, the PV modules produced the most, whereas in winter, in early afternoon, the modules produced the most. This is due to the fact that as the sun's angle varies during the day and year, so does the ideal tilt angle to obtain power from the module.

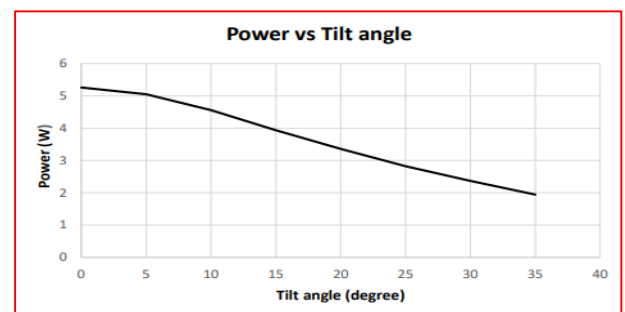


Figure 3.9 Variation of power with change in tilt angle

The performance of PV module with the variation in the temperature is shown in the figure 3.10. The obtained result showed that power decreases when temperature rises. This is due to the semiconductor material's broader bandgap energy at higher temperatures, which decreases efficiency and power output and the material's capacity to absorb solar light. The internal carrier recombination rates rise with temperature.

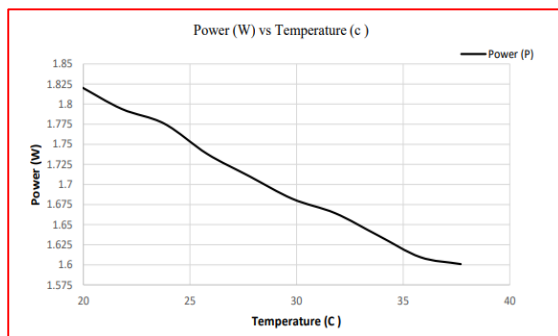


Figure 3.10: Power vs Temperature plot

IV. Real-Time Testing of Solar Modules:

Existing Setup Issues:

In the SEE 605 lab's experimental arrangement, 12 halogen lights, each with a power of 150W, were employed to mimic sunlight for experiments. However, a drawback was encountered due to fluctuations in radiation levels and the practical consideration of the sun's position, which changes with the day of the month and solar time.

Analysis for Improvement:

An enhancement can be achieved through real-time testing of solar tracking based on the geographical location, considering the day of the year and solar time. Various solar angles can be determined using the following parameters:

- Location on Earth's surface (Latitude angle, L)
- Day of the year (N value), e.g., N=10 for January 10

- Time of the day (solar time)

By utilizing these parameters, additional angles can be derived:

- **Declination angle (δ)** = $23.45 * \sin(360 * (284 + N) / 365)$
- **Hour Angle (h)** = $15 * (\text{Solar Time} - 12)$
- **Sun's Altitude Angle (β)** = $(\cos L * \cos h * \cos \delta) + (\sin L * \sin \delta)$
- **Solar Azimuth Angle (Φ)** = $\cos^{-1}((\sin \delta * \cos L) - (\cos \delta * \sin L * \cos h)) / \cos \beta$

The solar azimuth angle and sun's altitude angle play a crucial role in the analysis since these angles change based on the day of the year and the specific time of the day.

Selected Location: Kanpur

- Latitude angle: 26°N
- Longitude Angle: 80.33°E
- N values for different solstices and equinox:
- Summer solstice (21st June): 173
- Winter solstice (21st Dec): 355
- Equinox solstice (21st Mar or 21 Sept): 81 or 265

The variation of the declination angle over the year was initially plotted, as it changes according to the formula: Declination angle (δ) = $23.45 * \sin(360 * (284 + N) / 365)$. This angle represents the inclination between the line connecting the Earth's center to the sun and its projection on the equatorial plane, ranging from -23.45° to 23.45° . This information aids in calculating azimuth as well as altitude angles. Variation of declination angle with month has been shown in Fig 4.1

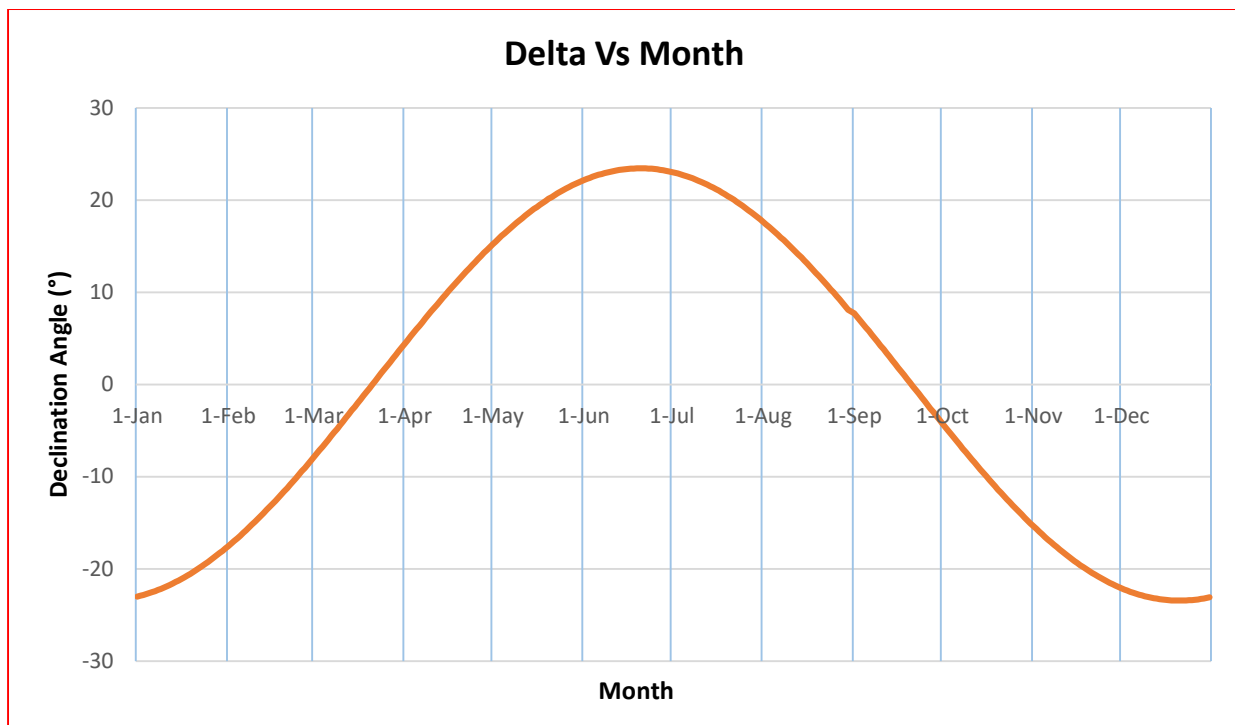


Figure 4.1: Declination angle Vs Month

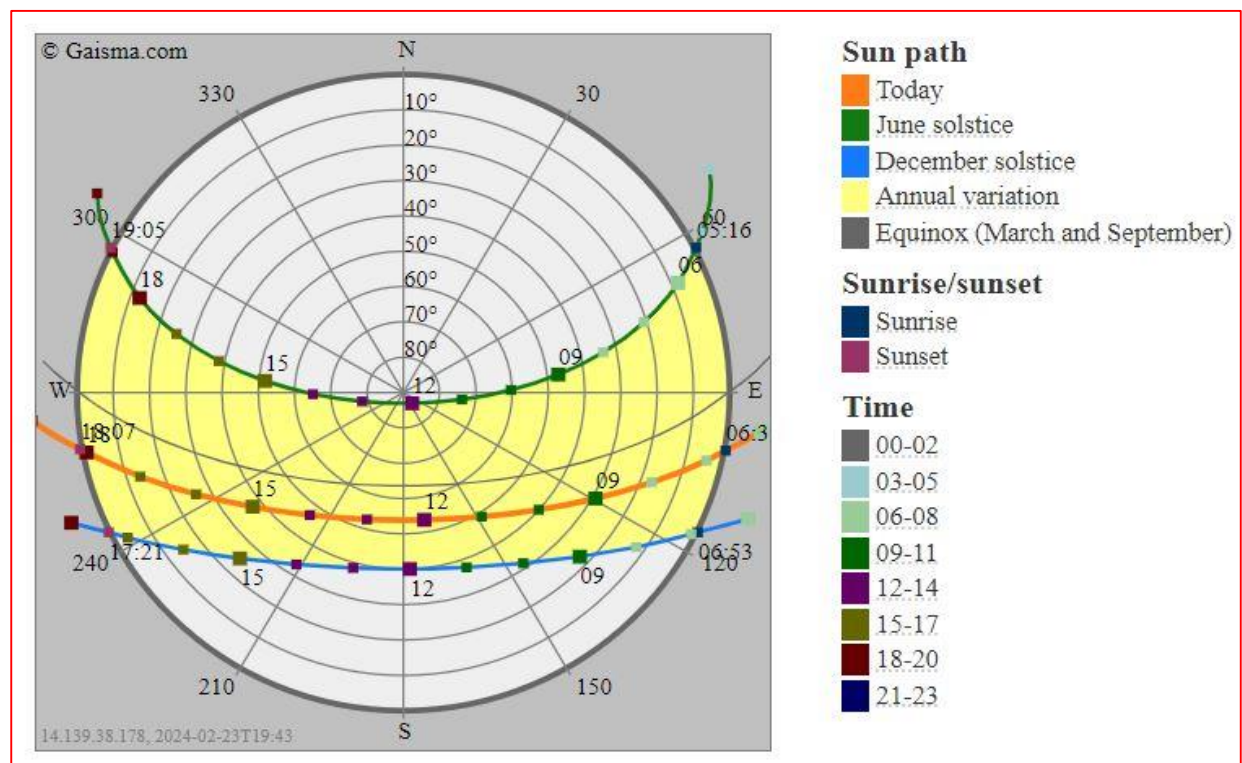
Sun Path diagram for Kanpur:

Figure 4.2 : Sun- path diagram for Kanpur (26.45°N)

Analysis for different seasons over the day:

1. Summer solstice (June 21):

Data table:

Time	Hour Angle(°), h	Sun Altitude Angle(°), β	Zenith Angle(°)	Solar Azimuth Angle(°), Φ
6:00 AM	-90	10.24246851	79.75753149	68.82553952
7:00 AM	-75	22.98832462	67.01167538	74.25834027
8:00 AM	-60	36.06659099	53.93340901	79.21032512
9:00 AM	-45	49.36333936	40.63666064	84.10634952
10:00 AM	-30	62.79032651	27.20967349	89.72817451
11:00 AM	-15	76.23667999	13.76332001	99.27214691
12:00 PM	0	87.6243624	2.375637597	141.7281745
1:00 PM	15	76.23667999	13.76332001	259.2721469
2:00 PM	30	62.79032651	27.20967349	269.7281745
3:00 PM	45	49.36333936	40.63666064	274.1063495
4:00 PM	60	36.06659099	53.93340901	279.2103251
5:00 PM	75	22.98832462	67.01167538	284.2583403
6:00 PM	90	10.24246851	79.75753149	288.8255395

3. Equinox (Mar 21):

Data Table:

Time	Hour Angle(°), h	Sun Altitude Angle(°), β	Zenith Angle(°)	Solar Azimuth Angle(°), Φ
6:00 AM	-90	0.03752545	89.96247455	0
7:00 AM	-75	12.32122993	77.67877007	40
8:00 AM	-60	24.30492739	65.69507261	80
9:00 AM	-45	35.57413669	54.42586331	120
10:00 AM	-30	45.42209433	44.57790567	140
11:00 AM	-15	52.59281569	37.40718431	160
12:00 PM	0	55.31734305	34.68265695	180
1:00 PM	15	52.59281569	37.40718431	195
2:00 PM	30	45.42209433	44.57790567	210
3:00 PM	45	35.57413669	54.42586331	225
4:00 PM	60	24.30492739	65.69507261	240
5:00 PM	75	12.32122993	77.67877007	255
6:00 PM	90	0.03752545	89.96247455	270

2. Winter Solstice (Dec 21):

Data Table:

Time	Hour Angle(°), h	Sun Altitude Angle(°), β	Zenith Angle(°)	Solar Azimuth Angle(°), Φ
7:00 AM	-75	2.07650126	87.92349874	117
8:00 AM	-60	13.5587897	76.4412103	124
9:00 AM	-45	23.8674772	66.1325228	133
10:00 AM	-30	32.3565317	57.64346825	145
11:00 AM	-15	38.1156397	51.88436035	160
12:00 PM	0	40.1835959	49.81640414	177
1:00 PM	15	38.1156397	51.88436035	195
2:00 PM	30	32.3565317	57.64346825	211
3:00 PM	45	23.8674772	66.1325228	223
4:00 PM	60	13.5587897	76.4412103	233
5:00 PM	75	2.07650126	87.92349874	238

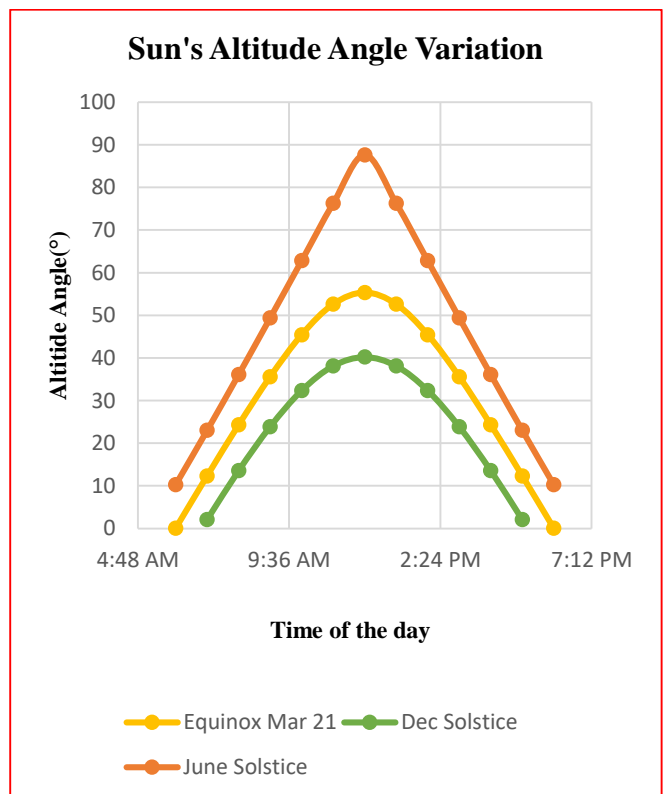


Figure 4.3: Altitude angle comparison for different seasons over the day

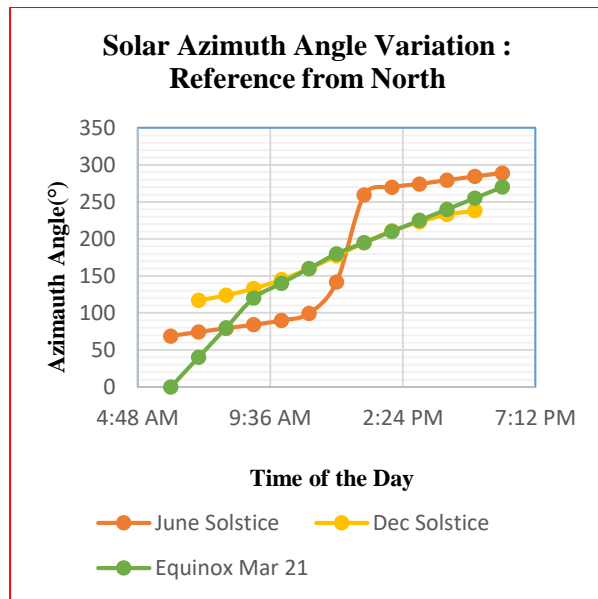


Figure 4.4: Solar azimuth angle comparison for different seasons over the day

Conclusion from the Graphs:

The analysis of altitude angle and solar azimuth angle graphs emphasizes the need for optimizing the orientation of Solar PV modules to achieve maximum output. Adapting the module's positioning in alignment with the sun's rays is crucial to ensure the highest incident radiation power, leading to maximum power output from the solar module or power plant.

Methodology:

To implement the findings from the conclusion and achieve optimal orientation, a Solar Angle Monitoring Control System is proposed. The main objective is to direct solar panels perpendicular to the sun's rays, and the methodology involves the following steps:

1. Solar Angle Monitoring Control System:

- Utilizes an AT89S52 microcontroller as the core control unit [7].

- Implements a simple yet effective control system for aligning panels with the sun on a single or double axis.
- Incorporates two photosensitive sensors (LDR) and a relay-based single-axis controllable solar tracking system operated by a servo motor.

2. MATLAB Software Integration:

- Monitors the entire control system through MATLAB software.
- Tailors the system for a specific location, such as Kanpur in this case [7].

3. Chronological Order in Solar Tracking:

- Implements a closed-loop tracking mechanism based on control principles with feedback.
- Utilizes a light sensor to detect the intensity of the sun's rays, serving as input to the control system.
- Employs the microcontroller to control the motion of the servo motor, adjusting the orientation of the module.
- Incorporates feedback to continuously compare the module's orientation with the sun's altitude and azimuth angles [7]

By employing this solar angle monitoring control system, solar panels can dynamically and autonomously adjust their orientation, ensuring optimal alignment with the sun throughout the day. This methodology enhances the overall efficiency and power output of the solar modules or solar power plants, contributing to a more effective utilization of solar energy resources.

Block diagram plotted using draw.io software has been shown in figure 4.5.

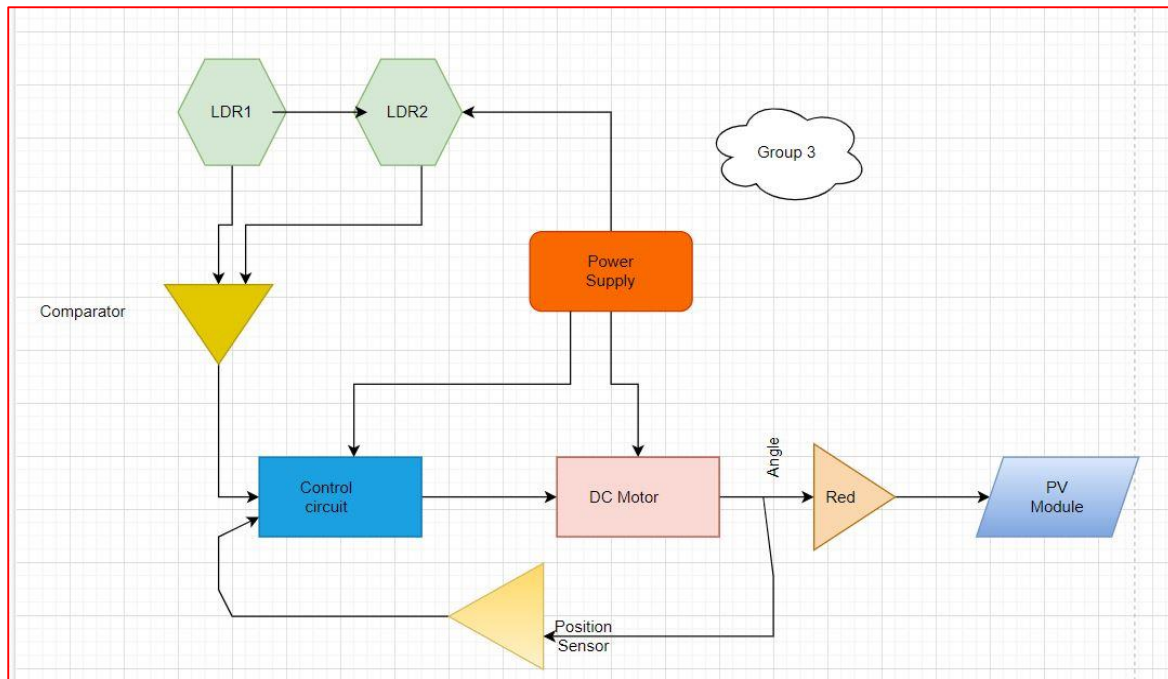


Figure 4.5: Block diagram of solar tracking control system

Mechanical components:

Swivel Mechanism: It will allow the rotation of the modules based upon the output of solar tracking control system. It has been shown in figure 4.6.



Figure 4.6: Swivel drive ball bearing

Input power on the solar module after monitoring solar angles:

- $G_{ND} (W/m^2) = A / \exp(B / \sin \beta)$
- G_{ND} = normal direct irradiation (W/m^2)
- A = apparent solar irradiation at air mass equal to zero (W/m^2)
- B = atmospheric extinction coefficient
- β = solar altitude,
- N = clearness number [assumed as 1]
- **Power Input = $G_{ND} \times (\text{Area of a module})$**

Time	$G_{ND} (W/m^2)$
6:00 AM	384.5991678
7:00 AM	679.0502364
8:00 AM	796.8733462
9:00 AM	855.2768733
10:00 AM	886.5937409
11:00 AM	902.4433038
12:00 PM	907.3870749
1:00 PM	902.4433038
2:00 PM	886.5937409
3:00 PM	855.2768733
4:00 PM	796.8733462
5:00 PM	679.0502364
6:00 PM	384.5991678

Summer Solstice

Time	G_{ND} (W/m ²)
7:00 AM	22.45720491
8:00 AM	602.8268266
9:00 AM	776.3372726
10:00 AM	845.2240629
11:00 AM	875.3553267
12:00 PM	884.072199
1:00 PM	875.3553267
2:00 PM	845.2240629
3:00 PM	776.3372726
4:00 PM	602.8268266
5:00 PM	22.45720491

Winter Solstice

Time	G_{ND} (W/m ²)
6:00 AM	1.9198E-100
7:00 AM	562.9800815
8:00 AM	798.7323045
9:00 AM	891.7438881
10:00 AM	936.3682669
11:00 AM	957.6519514
12:00 PM	964.0311196
1:00 PM	957.6519514
2:00 PM	936.3682669
3:00 PM	891.7438881
4:00 PM	798.7323045
5:00 PM	562.9800815
6:00 PM	1.9198E-100

Equinox

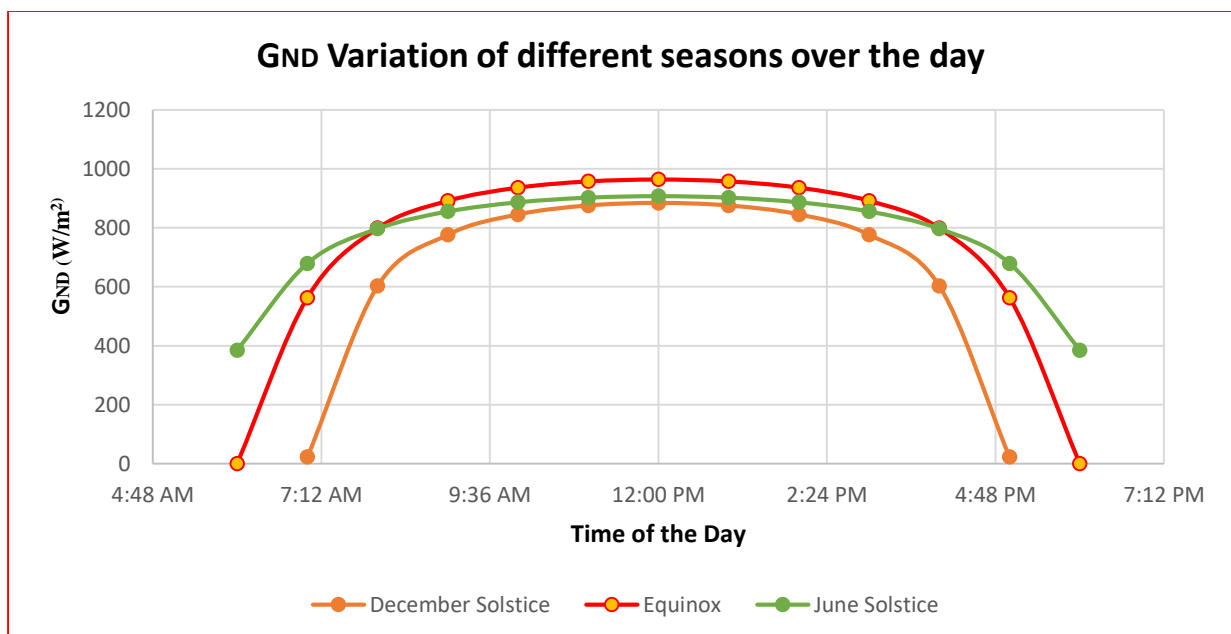
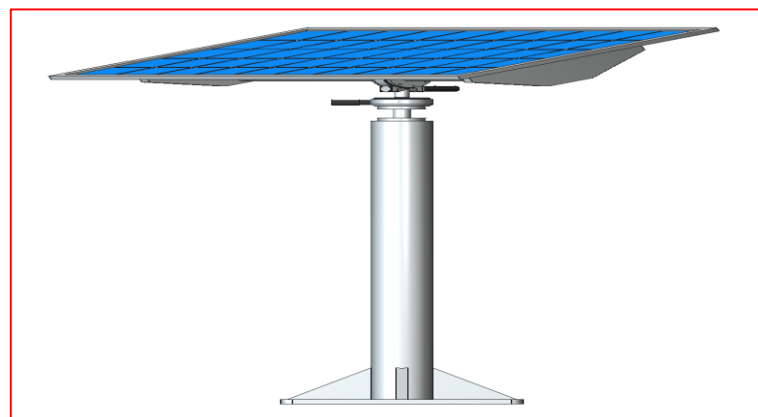
Figure 4.7: G_{ND} variation of different seasons over the day

Figure 4.8: Double Axis monitored Solar PV Module

Pros:

1. More Productivity:

- The proposed solar angle monitoring control system is anticipated to enhance efficiency significantly, with an expected increase of 30-40 percent when compared to static solar modules.

2. Easy Monitoring:

- The system offers convenient monitoring capabilities through a PC interface, providing real-time insights and control.

3. Land Optimization:

- Increased power output translates to higher efficiency, allowing for the generation of more power within a given area. This leads to better land optimization, as less land area is required to meet high power requirements.

Cons:

1. High Cost:

- The adoption of the proposed solar angle monitoring control system may involve a higher initial cost compared to conventional static systems. This cost factor should be considered in the overall economic analysis.

2. More Maintenance Required:

- The system may demand more maintenance compared to traditional setups. Regular checks and servicing are essential to ensure the continued optimal performance of the solar tracking mechanism.

3. Weather Conditions:

- Adverse weather conditions, particularly low clearness numbers (<1), could pose challenges for power output. Overcast skies or reduced sunlight intensity may affect the

system's ability to accurately track and adjust to the sun's position.

V. Conclusions:

In this investigation, a parametric analysis of solar PV modules has been conducted using a scaled-down solar power plant with artificial sunlight (Halogen lights). The objective is to gain insights into the fundamental physics of solar PV panels, encompassing I-V and P-V characteristics, fill factor, and efficiency. This foundational understanding is crucial for optimizing their practical applications. The study provides detailed insights into the I-V and P-V characteristics of a solar PV module under varying radiation levels, tilt angles, and temperatures through comprehensive testing.

The findings reveal a significant dependence of the efficiency and maximum power output of a solar module on radiation levels, tilt angles, and temperatures. The study emphasizes the necessity of striking a balance between maximizing power and efficiency. Consequently, optimizing these parameters can lead to substantial improvements in both power production and efficiency.

Regarding *real-time testing analysis*, it is concluded that photovoltaic tracker systems with appropriate control mechanisms play a pivotal role in enhancing electrical power generation, showing an increase of **22 to 56%** compared to fixed photovoltaic systems. The research field is evolving rapidly, with ongoing studies exploring advanced techniques such as artificial neural networks and fuzzy logic. These tools find application in various domains, with fuzzy logic controllers

being particularly instrumental in *tracking the maximum power point in a photovoltaic system*.

VI. Acknowledgement:

Appreciation is extended to the Department of Sustainable Energy Engineering for establishing the experimental setup in our laboratory. Special thanks go to Prof. Jishnu Bhattacharya and Prof. Sudarshan Narayana for their invaluable insights and guidance throughout the experiment. Recognition is also given to the teaching assistant, Rajbala Purnima Priya and Ashutosh Shandilya for providing valuable support during the experiment. Additionally, sincere thanks to Mr. Chandan Kumar, Mr. Ajay Singh Chauhan and Dr. Deepika Jhahhria for their efforts in setting up the system.

VII. References:

- [1] Hasan, D.S., Farhan, M.S. and ALRikabi, H.T., 2023, February. The effect of irradiance, tilt angle, and partial shading on PV performance. In *AIP Conference Proceedings* (Vol. 2457, No. 1). AIP Publishing.
- [2] Nasrin, R., Hasanuzzaman, M. and Rahim, N.A., 2018. Effect of high irradiation on photovoltaic power and energy. *International Journal of Energy Research*, 42(3), pp.1115-1131.
- [3] Makrides, G., Zinsser, B., Schubert, M. and Georghiou, G.E., 2013. Energy yield prediction errors and uncertainties of different photovoltaic models. *Progress in photovoltaics: research and applications*, 21(4), pp.500-516.
- [4] Mamun, M.A.A., Islam, M.M., Hasanuzzaman, M. and Selvaraj, J., 2022. Effect of tilt angle on the performance and electrical parameters of a PV module: Comparative indoor and outdoor experimental investigation. *Energy and Built Environment*, 3(3), pp.278-290.
- [5] Torres, J.P.N., Nashih, S.K., Fernandes, C.A. and Leite, J.C., 2018. The effect of shading on photovoltaic solar panels. *Energy Systems*, 9, pp.195-208.
- [6] Woyte A, Nijs J, Belmans R. Partial shadowing of photovoltaic arrays with different system configurations: literature review and field test results. *Solar Energy* 2003;74:217-33.
- [7] Solar Tracking System - an overview | ScienceDirect Topics. Available at: <https://www.sciencedirect.com/topics/engineering/solar-tracking-system>